High-Gain N-Face AlGaN Solar-Blind Avalanche Photodiodes Using a Heterostructure as Separate Absorption and Multiplication Regions *

Yin Tang(汤寅)[1], Qing Cai(蔡青)[1], Lian-Hong Yang(杨莲红)[2], Ke-Xiu Dong(董可秀)[3], Dun-Jun Chen(陈敦军)[1**], Hai Lu(陆海)[1], Rong Zhang(张荣)[1], You-Dou Zheng(郑有炓)[1]

[1]*Key Laboratory of Advanced Photonic and Electronic Materials, School of electronic Science and Engineering, Nanjing University, Nanjing 210093*

[2]*Department of Physics, Changji College, Changji 831100*

[3]*School of Mechanical and Electronic Engineering, Chuzhou University, Chuzhou 239000*

(Received 17 September 2016)

It is well known that Ⅲ-nitride semiconductors can generate the magnitude of MV/cm polarization electric field which is comparable with their ionization electric fields. To take full advantage of the polarization electric field, we design an N-face AlGaN solar-blind avalanche photodiode (APD) with an $Al_{0.45}Ga_{0.55}N/Al_{0.3}Ga_{0.7}N$ heterostructure as separate absorption and multiplication (SAM) regions. The simulation results show that the N-face APDs are more beneficial to improving the avalanche gain and reducing the avalanche breakdown voltage compared with the Ga-face APDs due to the effect of the polarization electric field. Furthermore, the $Al_{0.45}Ga_{0.55}N/Al_{0.3}Ga_{0.7}N$ heterostructure SAM regions used in APDs instead of homogeneous $Al_{0.45}Ga_{0.55}N$ SAM structure can increase significantly avalanche gain because of the increased hole ionization coefficient by using the relatively low Al-content AlGaN in the multiplication region. Meanwhile, a quarter-wave AlGaN/AlN distributed Bragg reflector structure at the bottom of the device is designed to remain a solar-blind characteristic of the heterostructure SAM-APDs.

PACS: 85.60.Dw, 85.60.Bt DOI: 10.1088/0256-307X/34/1/018502

Solid-state AlGaN avalanche photodiodes (APDs), with Al composition more than 40%, can realize high-sensitivity detection of solar-blind ultraviolet signals ($\lambda < 290$ nm) under strong background radiation without needing expensive and efficiency-limiting optical filters. Thanks to the remarkable advantages such as low operation voltages, high optical gain, small sizes, and intrinsic solar-blind characteristic,[1–3] the APDs based on $Al_xGa_{1-x}N$ alloy semiconductors can be a replacement for photomultiplier tubes which are usually fragile, bulky, and expensive.[4] The excellent advantages of AlGaN APDs allow them to use in many fields including missile warning and tracking, flame monitoring, ultraviolet astronomy and bioagent detection.[5]

Compared with visible-blind GaN APDs which have realized single photon detection under the Geiger mode operation,[6,7] so far only a few works on AlGaN solar-blind APDs have been reported and the multiplication gain of AlGaN solar-blind APDs has lagged far behind that of GaN APDs[8–10] due to the problems such as high dislocation density and low p-type doping efficiency.[11,12] The poor performances of the AlGaN solar-blind APDs have already blocked their applications.

It is well known that the spontaneous and piezoelectric polarization in Ⅲ-nitride can cause an electric field of up to several MV/cm, which is of the same order of magnitude as avalanche breakdown electric field in the multiplication region of AlGaN APDs.[13] Therefore, taking advantage of the polarization electric field reasonably can help to improve the performance of AlGaN APDs. In this Letter, to take full advantage of the polarization electric field, we design an N-face AlGaN solar-blind avalanche photodiode (APD) with $Al_{0.45}Ga_{0.55}N/Al_{0.3}Ga_{0.7}N$ heterostructure as separate absorption and multiplication (SAM) regions. Moreover, the use of relatively low Al-content $Al_{0.3}Ga_{0.7}N$ in the multiplication region can be conducive to increasing avalanche gain because of the increased hole ionization coefficient.[14] To keep the solar-blind characteristic of the designed APD, a quarter-wave distributed Bragg reflector (DBR) structure is also introduced.

Figure 1 shows the schematic structure of the N-face or Ga-face AlGaN heterostructure solar-blind SAM-APDs. The designed structure consists of an 800-nm-thick n-type $Al_{0.5}Ga_{0.5}N$ layer, a 180-nm-thick unintentionally doped $Al_{0.45}Ga_{0.55}N$ absorption layer, a 60-nm-thick composition graded n-AlGaN layer, a 140-nm-thick unintentionally doped $Al_{0.3}Ga_{0.7}N$ multiplication layer, and a 250-nm-thick p-type $Al_{0.3}Ga_{0.7}N$ layer. It can be predicted that the low-Al-content $Al_{0.3}Ga_{0.7}N$ layer may result in the loss of the solar-blind characteristic of the designed APD, thus we introduce a quarter-wave distributed Bragg reflector (DBR) structure between the n-type

*Supported by the State Key Project of Research and Development Plan of China under Grant No 2016YFB0400903, the National Natural Science Foundation of China under Grant Nos 61634002, 61274075 and 61474060, the Key Project of Jiangsu Province under Grant No BE2016174, the Anhui University Natural Science Research Project under Grant No KJ2015A153, and the Open Fund of State KeyLab of Optical Technologies on Nano-fabrication and Micro-engineering.

**Corresponding author. Email: djchen@nju.edu.cn

© 2017 Chinese Physical Society and IOP Publishing Ltd

$Al_{0.5}Ga_{0.5}N$ layer and the AlN template to make the APD remain a good solar-blind property. The conventional Ga-face homogeneous $Al_{0.45}Ga_{0.45}N$ SAM-APD is used here as a reference counterpart with a 60-nm-thick n-type charge layer, a 140-nm-thick multiplication layer and a 250-nm-thick p-type layer. For all of the APD structures, the hole-doping concentration for the p-type layer is $1 \times 10^{18}\,\mathrm{cm}^{-3}$, and the electron-doping concentrations are $1 \times 10^{18}\,\mathrm{cm}^{-3}$ and $2 \times 10^{18}\,\mathrm{cm}^{-3}$ for the n-type charge layer and the n-$Al_{0.5}Ga_{0.5}N$ layer, respectively. The residual carrier concentration for the unintentionally doped layers is $1 \times 10^{16}\,\mathrm{cm}^{-3}$.

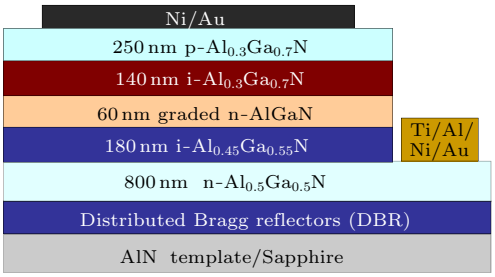

Fig. 1. Schematic structure of the N-face and Ga-face AlGaN heterostructure solar-blind SAM-APDs.

The voltage dependences of the photocurrent and dark current for back-illuminated N-face and Ga-face designed AlGaN APDs and conventional AlGaN APDs are calculated with the Silvaco Atlas software, as shown in Fig. 2. The calculated physical model and the parameters are the same as our previous work[15] except for the ionization coefficients which are extracted from Ref. [16]. In the simulation, the well-known Poisson equation and continuity equations are used. The physical models such as the carrier-concentration-dependent mobility model, the field-dependent mobility model, the SRH recombination model, the Auger recombination model, surface recombination and optical generation–recombination are taken into account. Four types of dark current mechanisms including diffusion current, generation–recombination current, band-to-band current, and trap-assistant tunneling current are also used for calculating the breakdown voltage and gain.[17] The wavelength and power density of incident light are 280 nm and $8 \times 10^{-5}\,\mathrm{W/cm}^{-2}$, respectively. The device size is $625\,\mu\mathrm{m}^2$. From Fig. 2, we can see that the photocurrents for Ga-face heterostructure and conventional APDs keep quite flat until the reverse bias increases to about 60 V where the ionization events start to happen. However, for N-face heterostructure APDs, when the reverse bias exceeds approximately 30 V, the current starts to increase exponentially. The calculated avalanche breakdown voltage and maximum multiplication gain for the three APDs are summarized in Table 1. The multiplication gain is taken as the difference of multiplied photocurrent and dark current normalized by the difference of unmultiplied photocurrent and dark current. The unmultiplied current is evaluated from the average value of the flat portion of the curves.[11] From Table 1, we can see that, for the N-face heterostructure APDs, the multiplication gain increases pronouncedly from 4.66×10^4 for the conventional APDs to 3.31×10^5, showing an increase about 710%, whereas the avalanche breakdown voltage is 30% lower than that of the conventional APDs. Furthermore, the N-face heterostructure APDs also show a lower avalanche breakdown voltage and a higher gain compared with the counterpart of the Ga-face APDs.

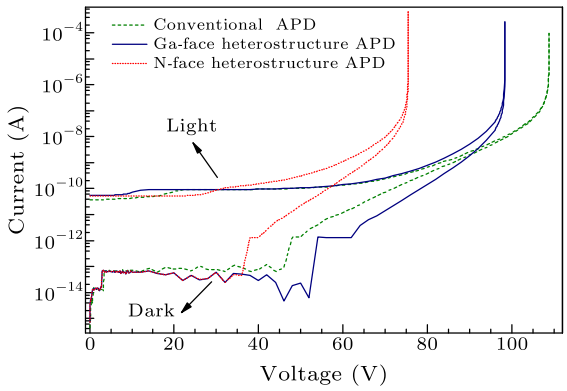

Fig. 2. Reverse I–V curves of the AlGaN APDs with different structures.

Table 1. Summary of avalanche breakdown voltage and maximum multiplication gain for the AlGaN APDs with different structures.

	Voltage (V)	Gain
Conventional APD	108.88	4.66×10^4
Ga-face heterostructure APD	98.37	1.51×10^5
N-face heterostructure APD	75.47	3.31×10^5

We simulate the electric field distributions of the N-face and Ga-face heterostructure APDs and the conventional AlGaN APD, as shown in Fig. 3. From Fig. 3(a), we find that the electric field strength in the multiplication layer of the N-face heterostructure APD is stronger than that of the Ga-face heterostructure APD at reverse bias of 0 V. We owe the increase of the electric field strength in the multiplication layer to a polarization-induced electric field, which has been widely studied in high electron mobility transistors.[18] It should be noted that the polarization charge densities in our calculation models are assumed to be 40% of the calculated values in the case of considering the screening effect caused by defects.[15] For the N-face heterostructure APD, due to the discrepancy of Al composition of the i-$Al_{0.3}Ga_{0.7}N$ layer and the n-type charge layer, a polarization field in the multiplication layer can be induced by the positive polarization charges at the interface of i-$Al_{0.3}Ga_{0.7}N$ and n-type charge layers, which is in the same direction of the reverse-bias field and built-in field, and thus enhances the total electric field in the multiplication layer. However, for the Ga-face heterostructure APD, the polarization-induced electric field in the multiplication layer with the direction opposite to the built-in electric field can weaken the total electric field in the multiplication

layer. The electric field strength in the multiplication layer of the heterostructure APD without taking the polarization field into account just falls between those of the Ga-face and N-face heterostructure APDs, which also confirms the contribution of the polarization field.

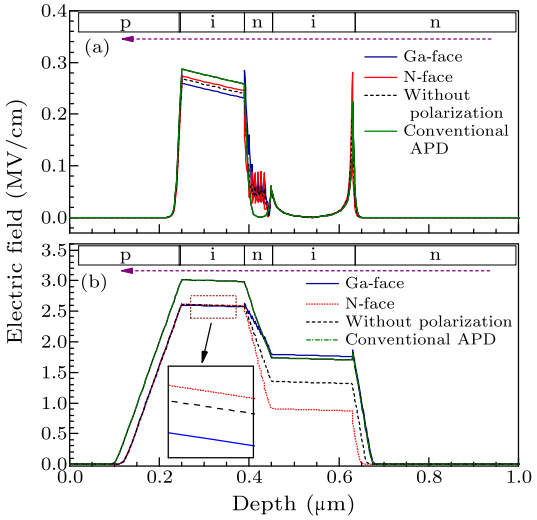

Fig. 3. The electric field distributions of the N-face and Ga-face heterostructure APDs, the heterostructure APD without taking polarization field into account and the conventional AlGaN APD at (a) reverse bias of 0 V, and (b) at the voltage point with maximum multiplication gain.

Moreover, we also calculate the electric field distributions at the voltage point with the maximum multiplication gain, as shown in Fig. 3(b). We can see that the total electric field in the multiplication layer for N-face and Ga-face heterostructure APDs is much lower than that in conventional AlGaN APDs, which can help to decrease the risk of premature breakdown. The required avalanche electric field decreases significantly at the low-Al-content $Al_{0.3}Ga_{0.7}N$ layer as expected, thanks to the reduced band gap, which is beneficial to obtain a higher gain. Further, the hole impact ionization coefficient increases remarkably with decreasing Al composition in the AlGaN alloys, according to Ref. [16] at least five times higher than that of using the low-Al-content $Al_{0.3}Ga_{0.7}N$ instead of the high-Al-content $Al_{0.45}Ga_{0.55}N$ as the multiplication layer. Thus both the Ga-face and the N-face heterostructure APDs can obtain a remarkably higher gain at a quite lower breakdown voltage compared with the conventional APD.

In addition, we can see that the N-face heterostructure APD has higher electric field strength in the multiplication region and a narrower depletion width in the n-type layer. It is well known that even a small enhancement of the electric field can also raise significantly the multiplication gain because of the exponential dependence of the impact ionization coefficient on the electric field.[19] This would explain why the N-face heterostructure APD has a 120% gain compared to the Ga-face heterostructure APD when using the same structure and parameters. Similar to Ref. [20], the positive polarization charge at the interface of the i-$Al_{0.3}Ga_{0.7}N$ and n-type charge layers serves to block the depletion region to extend toward the n-type layer and greatly reduces the electric field in the absorption region, which can confine more voltage drop in the multiplication region and hence can contribute to obtaining a lower avalanche breakdown voltage. Compared to the Ga-face heterostructure APD, by one rough estimation, the voltage drops in the absorption layer and the n-$Al_{0.5}Ga_{0.5}N$ layer of the N-face APD can be reduced by about 16 V and 4 V, respectively. The voltage drop in the n-type charge layer is also reduced though by a relatively smaller amount. The decrease of the breakdown voltage can contribute to a rise of the reliability of APDs and simplify the driver circuitry.[20,21]

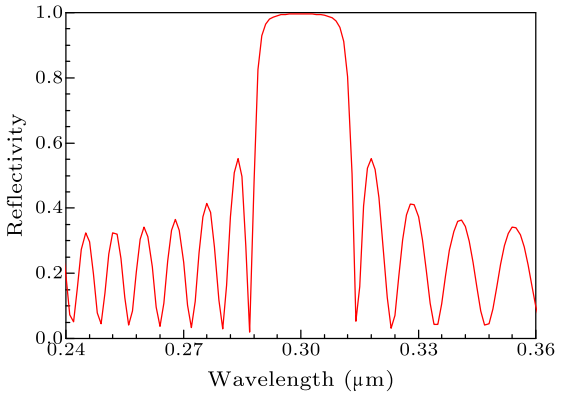

Fig. 4. Reflectivity spectra of the DBR structure.

However, use of the low-Al-content $Al_{0.3}Ga_{0.7}N$ layer in the multiplication region can have an impact on the solar-blind characteristic of the designed APDs. Thus we introduce a quarter-wave distributed Bragg reflector (DBR) structure between the n-$Al_{0.5}Ga_{0.5}N$ layer and the AlN template to keep the solar-blind characteristic. The designed DBR structure is made up of 27.5 pairs of $Al_{0.5}Ga_{0.5}N$/AlN periodic structure with a central wavelength of 300 nm. The thicknesses of AlN and $Al_{0.5}Ga_{0.5}N$ layers are 34.25 and 30.85 nm decided by the formula $d = \lambda/4n$. Here the refractive indices of AlN (2.190) and $Al_{0.5}Ga_{0.5}N$ (2.431) were extracted from Ref. [22]. Figure 4 shows the calculated reflectivity spectrum of the DBR structure by the transfer matrix method. It can be seen that the DBR maintains a high reflectance of 95%–99.9% in the wavelength range of 290–310 nm, where the long wavelength side of the high reflectance region just corresponds to the band gap energy of $Al_{0.3}Ga_{0.7}N$ alloy.

Figure 5 shows the spectral responsivities of the N-face heterostructure APDs in both cases with and without DBR structure at −30 V, where the ionization event has started. The spectral responsivity of the N-face heterostructure APD with DBR structure presents a sharp cutoff at 290 nm. The designed APD remains a good solar-blind characteristic thanks to the

high reflectivity of the DBR structure in the range of 290–310 nm. However, for the N-face heterostructure APD without the DBR structure, the cutoff wavelength of spectral responsivity shifts to 308 nm as expected, corresponding to the absorption edge of $Al_{0.3}Ga_{0.7}N$.

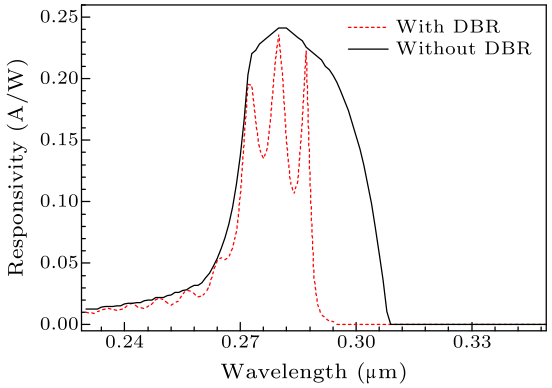

Fig. 5. Spectral responsivities of the N-face heterostructure APDs in both the cases with and without DBR structure at −30 V.

In summary, the performances of the N-face heterostructure AlGaN solar-blind SAM-APD have been studied theoretically. The simulation results show that the N-face heterostructure APDs can obtain a lower avalanche breakdown voltage and a higher gain compared with the Ga-face APDs thanks to the effect of the polarization electric field. Moreover, using the relatively low-Al-content $Al_{0.3}Ga_{0.7}N$ in the multiplication region can help to increase avalanche gain due to the higher hole ionization coefficient. Meanwhile, introducing the DBR structure in the bottom of the device can insure the good solar-blind characteristic of the designed APDs.

References

[1] Yoo D, Limb J, Ryou J, Zhang Y, Shen S, Dupuis R, Hanser D, Preble E and Evans K 2007 *IEEE Photon. Technol. Lett.* **19** 1313
[2] Huang Y, Chen D J, Lu H, Dong K X, Zhang R, Zheng Y D, Li L and Li Z H 2012 *Appl. Phys. Lett.* **101** 253516
[3] Wang X D, Hu W D, Pan M, Hou L W, Xie W, Xu J T, Li X Y, Chen X S and Lu W 2014 *J. Appl. Phys.* **115** 013103
[4] Shao Z G, Chen D J, Lu H, Zhang R, Cao D P, Luo W J, Zheng Y D, Li L and Li Z H 2014 *IEEE Electron Device Lett.* **35** 3
[5] Bulmer J, Suvarna P, Leathersich J, Marini J, Mahaboob I, Newman N and Shadi F 2016 *IEEE Photon. Technol. Lett.* **28** 1
[6] Carrano J C, Lambert D J H, Eiting C J, Collins C J, Li T, Wang S, Yang B, Beck A L, Dupuis R D and Campbell J C 2000 *Appl. Phys. Lett.* **76** 7
[7] Choi S, Kim H, Zhang Y, Bai X, Yoo D, Limb J, Ryou J, Shen S, Yoder P D and Dupuis D 2009 *IEEE Photon. Technol. Lett.* **21** 1526
[8] Mcclintock R, Yasan A, Minder K, Kung P and Razeghi M 2005 *Appl. Phys. Lett.* **87** 241123
[9] Tut T, Gokkavas M, Inal A and Ozbay E 2007 *Appl. Phys. Lett.* **90** 163506
[10] Huang Z Q, Li J F, Zhang W L and Jiang H 2013 *Appl. Phys. Express* **6** 054101
[11] Sun L, Chen J L, Li J F and Jiang H 2010 *Appl. Phys. Lett.* **97** 191103
[12] Yang B, Li T, Heng K, Collins C, Wang S, Carrano J C, Dpuis R D, Campbell J C, Schurman M J and Ferguson I T 2000 *IEEE J. Quantum Electron.* **36** 12
[13] Zhang S K, Wang W B, Dabiran A M, Osinsky A, Wowchak A M, Hertog B, Plaut C, Chow P P, Gundry S, Troudt E O and Alfano R R 2005 *Appl. Phys. Lett.* **87** 262113
[14] Bertazzi F, Moresco M and Bellotti E 2009 *J. Appl. Phys.* **106** 063718
[15] Dong K X, Chen D J, Lu H, Liu B, Han P, Zhang R and Zheng Y D 2013 *IEEE Photon. Technol. Lett.* **25** 1510
[16] Bellotti E, Bertazzi F, Shishehchi S, Matsubara M and Goano M 2013 *IEEE Trans. Electron Devices* **60** 3204
[17] Wang X D, Hu W D, Chen X S, Xu J T, Wang L, Li X Y and Lu W 2011 *J. Phys. D* **44** 405102
[18] Ambacher O, Foutz B, Smart J, Shealy J R, Weimann N G, Chu K, Murphy M, Sierakowski A J, Schaff W J, Eastman L F, Dimitrov R, Mitchell A and Stutzmann M 2000 *J. Appl. Phys.* **87** 1
[19] Wu L L, Zhao D G, Deng Y, Jiang D S, Zhu J J, Wang H, Liu Z S, Zhang S M, Zhang B S and Yang H 2012 *Sci. Chin. Phys. Mech. Astron.* **55** 619
[20] Bulmer J, Suvarna P, Leathersich J, Marini J, Mahaboob I, Newman N and Shahedipour-Sandvik F 2016 *IEEE Photon. Technol. Lett.* **28** 1
[21] Verghese S, McIntosh K A, Molnar R J, Mahoney L J, Aggarwal R L, Geis M W, Molvar K M, Duerr E K and Melngailis I 2001 *IEEE Trans. Electron Devices* **48** 3
[22] Brunner D, Angerer H, Bustarret E, Freudenberg F, Hopler R, Dimitrov R, Ambacher O and Stutzmann M 1997 *J. Appl. Phys.* **82** 5090